

Fatigue 2010

## Two-scale model of low-cycle fatigue. Embrittlement of pre-fracture zone material

Vladimir M. Kornev \*

*Lavrentyev Institute of Hydrodynamics, Lavrentyev avenue, 15, Novosibirsk, 630090, Russia*

Received 26 February 2010; revised 9 March 2010; accepted 15 March 2010

---

### Abstract

A model describing extension of the crack tip in low-cycle fatigue is proposed. This model is appropriate to the scheme by Laird and Smith and describes occurrence of striations in fatigue. The material is considered as composed of quasi-brittle fibers with thin layers. The initial mode I macrocrack is located perpendicular to the fibers. The necessary and sufficient criteria of non-local fracture at the generalized stress state are used. The detailed information on material strain in the prefracture zone is obtained: processes of formation of earing, healing of thin layer material, accumulation of damages in the fibers, extension of the crack tip in discrete steps, and failure of specimens are described.

© 2010 Published by Elsevier Ltd. Open access under [CC BY-NC-ND license](#).

*Keywords:* Quasi-brittle, quasi-ductile material; fracture; necessary and sufficient criteria; damage; critical fracture parameters

---

### 1. Introduction

“The most characteristic feature of fracture surface microrelief of aluminum and titanium alloys, copper, iron, some steels, as well as of other metals and alloys are fatigue striations oriented perpendicular to the direction of crack extension. It is considered that the next striation is formed due to stoppage of a fatigue crack after each loading cycle” (see [1], p.136). It will be shown below that the next striation can be formed not only after each loading cycle, but after several loading cycles. Consider in more detail the Laird – Smith model [2, 3] of formation of striations.

### 2. Description of characteristics of structured metal under monotonous loading

Consider the macrocrack propagation in high stress fatigue when tensile pulsating loading is assigned. Ductile structured metals are under consideration. The excellent scheme illustrating the fracture process of such structured materials with relation to the scale of sizes is given in Fig. 3.1 of review by McClintock and Irwin [4]. Make use of this scheme. Pay attention to the intragrain cleavage and intergranular shear in a structured material. The simplest material structure is considered that allows the Laird – Smith model to be implemented. This structure consists of

---

\* Corresponding author. Tel.: +7-383-333-1746 ; fax: +7-383-333-1612.

E-mail address: [kornev@hydro.nsc.ru](mailto:kornev@hydro.nsc.ru)

unidirectional fibers separated by thin layers. Let the macrocrack be directed across the fibers. The fibers of material model sub-grains ( $\sim 10^{-2}$  cm) and thin layers between fibers model areas corresponding to sub-grain boundaries ( $\sim 10^{-4}$  cm). Implementation of the Laird – Smith model is significantly influenced by material characteristics. These characteristics have to describe just as microplasticity, so healing of material of thin layers at the first stage of tension, as well as the process of embrittlement under inelastic strain of both fibers and thin layers at the second stage of tension. Assign the first number to the fiber material and the second number to the thin layer material (subscripts); the initial state of material (at the time of delivery) is labeled by zero lower index, the state of material after the first, second, and etc. inelastic strain are labeled by one, two, and etc. (superscripts, the upper zero index can be omitted).

### Nomenclature

$G$	shear modulus
$K_I, K_{II}$	stress intensity factors (SIFs)
$N$	number of cycles
$V$	mean rate of macrocrack tip extension per one cycle
$Oxy, Or\theta$	Cartesian and polar coordinate systems
$a$	prefracture zone width
$f = f(\varphi)$	theoretical strength curves of Coulomb-Mohr type
$n, k$	integers
$r_i$	specific linear sizes $i = 1, 2$
$2v, 2u$	crack opening and crack flank displacement
$\mathbf{e} = (\varepsilon; \gamma), \mathbf{s} = (\sigma; \tau)$	strain and stress vectors
$\varepsilon, \gamma$	elongation and relative shear
$\Delta$	prefracture zone length
$\varphi, \theta$	polar angles
$\mu$	Poisson's coefficient
$\sigma, \tau$	normal and shear stresses
$\sigma_m, \tau_m$	theoretical (ideal) material strengths under tension and shear

Fig. 1 displays four theoretical strength curves of the Coulomb-Mohr type for two different isotropic materials. Curves 1 and 3 describe behavior of the first and the second materials in the initial state, and curves 2 and 4 describe behavior of the first and the second materials after inelastic strain; these curves in the polar coordinate system can be written in the form  $f_i = f_i(\varphi)$ . The proportional loading path is pointed by arrow 5 along which  $\sigma / \tau = c_0 = \text{const}$ , this proportional loading can be determined by the angle  $\varphi$  in the imaginary plane  $\sigma - \tau$ , where  $\sigma$  and  $\tau$  are normal and shear stresses.

Since the transition from quasi-ductile to quasi-brittle fracture will be discussed below, we elucidate this passage. The relative estimates of theoretical tensile  $\sigma_m$  and shear  $\tau_m$  strengths in the limiting cases are as follows: 1. for

materials inclined to cleavage, we have  $\sigma_m \approx \tau_m$ ; 2. for materials poorly resistant to dislocation emission, we have  $\sigma_m \gg \tau_m$ . Attention should be paid to the fact, that after inelastic strain of the initial material, the fracture type can change from the quasi-ductile type to the brittle one. Fig. 1 displays four curves of the theoretical strength: curve 1 describes quasi-ductile behavior of the second material since  $\sigma_{m2} \gg \tau_{m2}$ ; curves 2, 3, and 4 describe quasi-brittle behavior of both the first material before and after inelastic strain and the second material after inelastic strain since  $\sigma_{m2}^{(1)} \approx \tau_{m2}^{(1)}$ ,  $\sigma_{m1} \approx \tau_{m1}$ ,  $\sigma_{m1}^{(1)} \approx \tau_{m1}^{(1)}$ .

Now we consider  $s$ – $e$  diagrams of materials for the proportional loading path. Assume that stress vector  $\mathbf{s} = (\sigma; \tau)$  and strain vector  $\mathbf{e} = (\varepsilon; \gamma)$  are coaxial, i.e.,  $\varepsilon/\gamma = c_0 = \text{const}$ . These vectors have modules  $s = |\mathbf{s}| = \sqrt{\sigma^2 + \tau^2}$ ,  $e = |\mathbf{e}| = \sqrt{\varepsilon^2 + \gamma^2}$ . The considered  $s$ – $e$  diagrams are analogous to the classical  $\sigma$ – $\varepsilon$  diagrams. Fig. 2 displays the simplest approximations of  $s$ – $e$  diagrams for two materials: curve 1 is the  $s$ – $e$  diagram for the first material, curve 2 is the  $s$ – $e$  diagram for the second material in the presence of one small region of microplasticity and one healing. If curve 1 consists of two rectilinear segments, then curve 2 consists of four rectilinear segments. For  $s$ – $e$  diagrams, the following designations are used:  $s_{m1}, s_{m2}$  are theoretical (ideal) strengths of the first and the second materials, respectively, in the initial state;  $e_{01}, e_{02}$  are limiting elongations of the first and the second materials, respectively, in the zone of elastic strain;  $e_{11}$  is the maximum inelastic elongation of the first material;  $e_{12}$  is the maximum inelastic elongation of the second material in healing of damages;  $s_{m2}^{(1)}$  is the theoretical material strength after healing;  $e_{02}^{(1)}$  is the limiting elongation of the second material in the zone of elastic strain after healing;  $e_{12}^{(1)}$  is the maximum inelastic elongation of the second material after healing of damages.

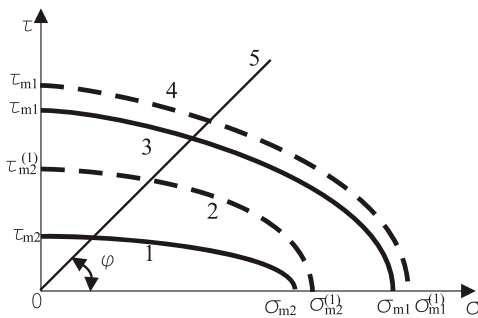


Fig. 1. Curves of theoretical strength of Coulomb-Mohr type

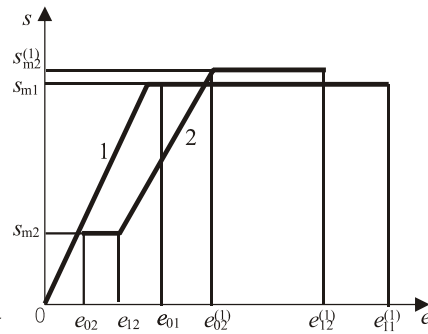


Fig. 2. Schematic  $s$ – $e$  diagrams for materials

Attention is drawn to the behavior of materials in the vicinity of points  $(s_{m1}, e_{11})$ ,  $(s_{m1}^{(1)}, e_{12}^{(1)})$  and the point  $(s_{m2}, e_{12})$ . If the first two points correspond to the process of fracture of the first and the second materials, then the third point corresponds to healing of the second material (thin layer material).

Laird and Smith [2] observed micro-hardness of material in the neighborhood of crack tips. Change in the hardness of materials results in their embrittlement. The proposed model of strain of fibers with thin layers includes parameters, which are capable of describing the process of embrittlement of materials. In the chosen model of material strain, by embrittlement is meant two different phenomena:

1. brittle-ductile transition, which is governed by the relations for the first material and for the second material

$$\tau_{m1}^{(1)} / \sigma_{m1}^{(1)} > \tau_{m1}^{(0)} / \sigma_{m1}^{(0)}, \quad \tau_{m1}^{(1)} / \sigma_{m1}^{(1)} \approx 1, \quad \tau_{m1}^{(0)} / \sigma_{m1}^{(0)} \approx 1, \quad (1)$$

$$\tau_{m2}^{(1)} / \sigma_{m2}^{(1)} > \tau_{m2}^{(0)} / \sigma_{m2}^{(0)}, \quad \tau_{m2}^{(1)} / \sigma_{m2}^{(1)} \approx 1, \quad \tau_{m2}^{(0)} / \sigma_{m2}^{(0)} \ll 1. \quad (2)$$

2. decrease in the maximum of inelastic elongation under repeated inelastic strains

$$e_{11}^{(j+1)} < e_{11}^{(j)}, e_{12}^{(j+2)} < e_{12}^{(j+1)} \text{ for } j = 0, 1, 2, 3, \dots \quad (3)$$

Imposition of limitations (1) for the first material induces the opening mode (mode I) crack to propagate rectilinearly just before and after inelastic strain. Imposition of limitations (2) for the second material induces the opening mode crack to propagate rectilinearly after inelastic strain only, and in the initial state, the behavior of material under fracture is quasi-ductile.

### 3. Model of crack tip extension under monotonous loading

We assume that i) the initial inner macrocrack is a sharp crack, and its right and left tips are located at boundaries between a fiber and a thin layer (further the region adjacent to the right tip is considered), ii) ahead of the macrocrack tip, the material is not deformed, and iii) all extensions of the macrocrack tip are considered as quasi-static.

#### 3.1. Crack branching angles

Assume that the material is isotropic. Consider the brittle fracture discrete-integral criterion of the Neuber-Novozhilov type for crack extension in the chosen directions  $\pm\theta$  defined by the branching angles

$$\langle \sigma_{\theta i}(\theta) \rangle = \frac{1}{n_i r_i} \int_0^{n_i r_i} \sigma_{\theta i}(r, \theta) dr \leq \sigma_i^*, \quad \langle \tau_{r\theta i}(\theta) \rangle = \frac{1}{n_i r_i} \int_0^{n_i r_i} \tau_{r\theta i}(r, \theta) dr \leq \tau_i^*, \quad n_i = 1, 2, \quad i = 1, 2. \quad (4)$$

Here  $Or\theta$  is the polar coordinate system;  $\sigma_{\theta i}(r, \theta)$  and  $\tau_{r\theta i}(r, \theta)$  are normal and shear stresses, respectively, possessing integrable singularity;  $\langle \sigma_{\theta i}(\theta) \rangle$  and  $\langle \tau_{r\theta i}(\theta) \rangle$  are averaged normal and shear stresses in the first  $i = 1$  or the second  $i = 2$  materials; notations  $\sigma_i^* = f_i(\varphi) \cos \varphi$  and  $\tau_i^* = f_i(\varphi) \sin \varphi$  are used for stresses of critical states (Fig. 1). Emphasize that left sides of the first and the second relations (4) are functions of the angle  $\theta$ , and right sides of the same relations are functions of the angle  $\varphi$ . For opening mode cracks (mode I), the relation between these angles was derived earlier  $\varphi = \theta/2$  (see [5, 6]). For the chosen structure of initial composite material (unidirectional fibers separated by thin layers), we have  $r_1 \gg r_2$ , in this case,  $r_1 = 10^{-2}$  cm and  $r_2 = 10^{-4}$  cm are specific linear sizes of the first and second material structure, respectively, [7]. Any damages are absent in the first and second materials. The first and the second relations from (4) are equivalent if the proportional loading  $\sigma_{\theta} / \tau_{r\theta} = c_0 = \text{const}$  takes place. When averaged stresses  $\langle \sigma_{\theta}(\theta) \rangle$  and  $\langle \tau_{r\theta}(\theta) \rangle$  coincide with stresses of the critical states  $\sigma^*, \tau^*$ , i.e.,  $\langle \sigma_{\theta}(\theta) \rangle = \sigma^*$  and  $\langle \tau_{r\theta}(\theta) \rangle = \tau^*$ , the criterion (4) is hold in the chosen directions  $\pm\theta^*$ . A single prefracture zone is formed on the crack continuation if  $\theta^* = 0$ , and two prefracture zones are formed when branching of the inner crack of the length  $2l$  takes place if  $\theta^* \neq 0$ .

Assume that quasi-brittle fracture takes place in fibers of the first material before and after inelastic deformation owing to the fact that restrictions (1) are imposed, then  $\varphi_1^* = \theta_1^* = 0$ .

Let in the thin layer from the second material i) quasi-ductile fracture takes place in the initial state because of the third inequality from (2) is hold, then  $\varphi_2^* = \theta_2^* / 2 \approx \pi/4$ , ii) after inelastic deformation, quasi-brittle fracture takes place because of the first and second restrictions from (2) are imposed, then  $\varphi_2^* = \theta_2^* = 0$ . The thin layer  $r_2 \ll r_1$  from the second material in the initial state poorly resists to the shear  $\tau_{m2} \ll \sigma_{m2}$  (see [6]).

### 3.2. Sufficient fracture criterion at generalized stress state

In order to describe fracture with account of damage accumulation in the prefracture zone, it is expedient to make use of the sufficient fracture criterion [8, 9]. This sufficient criterion is conveniently presented in the Cartesian coordinate system  $Oxy$  when the right tip of a crack branch coincides with the origin and  $Ox$ -axis is directed along this branch. Thus, the prefracture zone occupies the area, the length of which is equal to the length of the branch. Denote by  $\Delta$  the prefracture zone length and by  $a$  the prefracture zone width. The sufficient criterion for a sharp crack has the form

$$\frac{1}{k_i r_i} \int_0^{n_i r_i} \sigma_{yi}(x, 0) dx \leq \sigma_i^*, \quad \frac{1}{k_i r_i} \int_0^{n_i r_i} \tau_{xyi}(x, 0) dx \leq \tau_i^*, \quad x \geq 0, \quad i = 1, 2, \quad (5)$$

$$2v_i(-\Delta_i) = \frac{\eta+1}{G} K_I \sqrt{\frac{\Delta_i}{2\pi}} \leq 2v_i^*, \quad 2u_i(-\Delta_i) = \frac{\eta+1}{G} K_{II} \sqrt{\frac{\Delta_i}{2\pi}} \leq 2u_i^*, \quad -\Delta_i \leq x \leq 0, \quad i = 1, 2. \quad (6)$$

Here  $\sigma_{yi}(x, 0)$  and  $\tau_{xyi}(x, 0)$  are normal and shear stresses, respectively;  $n_i$  and  $k_i$  are integers ( $n_i \geq k_i$ ,  $k_i$  is the number of damage-free elements of the material structure);  $n_i r_i$  are averaging intervals for the first  $i=1$  and the second  $i=2$  materials;  $2v_i = 2v_i(x)$  and  $2u_i = 2u_i(x)$  are crack opening and crack flank displacement, respectively;  $2v_i^*$  and  $2u_i^*$  are critical crack opening and critical crack flank displacement, respectively;  $\eta = 3 - 4\mu$  and  $\eta = (3 - \mu)/(1 + \mu)$  for plane strain and plane stress state, respectively, where  $\mu$  is Poisson's coefficient;  $G$  is the shear modulus;  $K_I$  and  $K_{II}$  are total SIFs in the generalized Leonov-Panasyuk-Dugdale model

$$K_I = K_{I\infty} + K_{I\Delta}, \quad K_{II} = K_{II\infty} + K_{II\Delta}. \quad (7)$$

Here  $K_{I\infty}$  and  $K_{II\infty}$  are SIFs generated by stresses  $\sigma_\infty$  and  $\tau_\infty$  given at infinity;  $K_{I\Delta}$  and  $K_{II\Delta}$  are SIFs generated by stresses  $\sigma_{mi}$  and  $\tau_{mi}$  acting in accordance with the generalized Leonov-Panasyuk-Dugdale model. The scheme of force loading in the generalized Leonov-Panasyuk-Dugdale model for the right crack branch occupied by prefracture zone is given in Fig. 3. Emphasize that the prefracture zone length  $\Delta$  is determined when solving a fracture problem (5), (6), and the prefracture zone width  $a$  is found from some additional characteristics for material each. From Novozhilov's nomenclature [10], criteria (4) and (5), (6) are the necessary and sufficient fracture criteria.

The system of the first relations for the criterion (5), (6) is equivalent to the system from the second relations for the criterion (5), (6) if proportional loading takes place, and stress and strain tensors are coaxial [8].

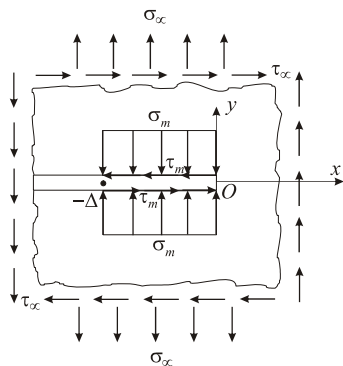


Fig. 3. Loading scheme in generalized model

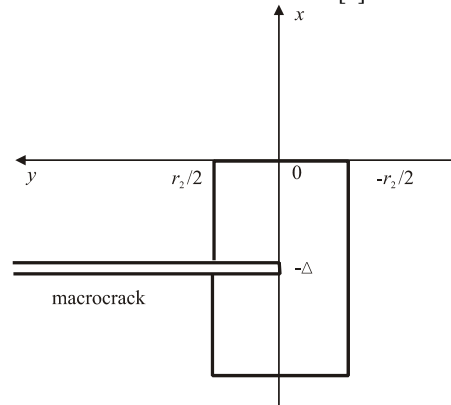


Fig. 4. Location of prefracture zones in thin layers

### 3.3. Healing of microcrack of the generalized shear

At first, fracture of a thin layer is considered, material of the layer being in the initial state, i.e.,  $i = 2$  in criteria (4) and (5), (6). Let at the generalized shear, the necessary criterion (4) be hold for the thin layer material, then for the quasi-ductile fracture, we have  $\theta_2^* \approx \pm\pi/2$  ( $\varphi_2^* \approx \pm\pi/4$ ). For the mode I microcrack for  $\theta_2^* = \pi/2$ , the following relations for the generalized shear are derived (see [6])

$$\tau_{r\theta_2}(r, \pi/4) / \sigma_{\theta_2}(r, \pi/4) = \langle \tau_{r\theta_2}(r, \pi/4) \rangle / \langle \sigma_{\theta_2}(r, \pi/4) \rangle = 1 \text{ for } \theta_2^* = \pi/2. \quad (8)$$

Thus, fracture ears occur in the thin layer (the second material) at right angles  $\theta_2^* = \pm\pi/2$  to the macrocrack plane.

We shall have to clear up what is the length of these ears. To do this, we make use of the sufficient criterion (5), (6) for the second material. Determine parameters of the critical opening  $2v_2^*$  of the microcrack and critical displacements  $2u_2^*$  of microcrack flanks. These critical parameters are determined through the prefraction zone width. Assume that the plasticity zone width in the second material exceeds the layer thickness, then the prefraction zone width for the second material coincides with the layer thickness, i.e. prefraction zones in the second material occupy rectangles with sides  $\Delta_2$  and  $a_2 = r_2$ , (Fig. 4). With account for microplastic peculiarities of the second material, the critical macrocrack opening and critical crack flank displacement are written in the form

$$2v_2^* = r_2(\varepsilon_{12} - \varepsilon_{02}), \quad 2u_2^* = r_2(\gamma_{12} - \gamma_{02}). \quad (9)$$

SIFs at the crack tips under uniaxial tension in the plane with the macrocrack having infinitesimal branches for  $\theta_2^* = \pm\pi/2$  can be written in accordance with handbook [11] in the form

$$K_{I\infty 2} = 0.372\sigma_\infty\sqrt{\pi l_0}, \quad K_{II\infty 2} = 0.348\sigma_\infty\sqrt{\pi l_0}. \quad (10)$$

From relation (7), SIFs  $K_{I\Delta}$  and  $K_{II\Delta}$  generated by stresses  $\sigma_{mi}$  and  $\tau_{mi}$  can be given in the form

$$K_{I\Delta} = K_{I\Delta}(\sigma_{m2}, l_0, \Delta/l_0, \theta_2^*), \quad K_{II\Delta} = K_{II\Delta}(\tau_{m2}, l_0, \Delta/l_0, \theta_2^*). \quad (11)$$

We failed to find the explicit type of relations (11) in handbooks. Let  $K_{I\Delta}$  and  $K_{II\Delta}$  be calculated for particular values of  $\sigma_{m2}, l_0, \Delta/l_0, \theta_2^*$  and  $\tau_{m2}, l_0, \Delta/l_0, \theta_2^*$ . Further we consider the first class of solutions when the total SIFs  $K_I$  and  $K_{II}$  in relations (7) are positive, i.e.,  $K_I = K_{I\infty} + K_{I\Delta} > 0$  and  $K_{II} = K_{II\infty} + K_{II\Delta} > 0$ . Then for the second material, all parameters of criterion (5), (6) are determined by relations (7), (9)-(10). After appropriate transformations of system from the first or the second relations for criterion (5), (6), critical parameters  $\sigma_{\infty 2}^*$ ,  $\Delta_2^*$  or  $\tau_{\infty 2}^*$ ,  $\Delta_2^*$  are found.

The obtained critical parameters of the load  $\sigma_{\infty 2}^*$  and the prefraction zone length  $\Delta_2^*$  describe occurrence of fracture ears for the initial plastic deformation at the crack tip. After deformation ears are formed, healing of the second material takes place after completion of the process of microplasticity at the generalized shear (8) at the point  $(s_{m2}, e_{12})$  in accordance with the  $s-e$  diagram in Fig. 2. Propagation of a crack of the generalized shear in the second material stops due to healing after relations (9) are hold. The critical opening  $2v_2^*$  of the macrocrack and the critical displacement  $2u_2^*$  of macrocrack flanks are responsible for occurrence of striations. Specific sizes of these striations are determined by relations (9) at the generalized shear and those are intimately related to characteristics of microplasticity of thin layer material. The mode I macrocrack is blunted because of  $2u_2^* \neq 0$  at the microscale, this blunting being commensurable with the specific linear size  $r_2$ .

### 3.4. Prefracture zone of macrocrack under monotonous loading

When fracture of the first and the second materials (i.e., materials of fibers and thin layers) ahead of the sharp crack is described, attention should be paid to the full plastic strain with embrittlement of material of fibers and thin layers. This results in accumulation of damages in the prefracture zone. Owing to the fact that quasi-brittle fracture takes place in the fiber material just as before, so after inelastic strain, and quasi-brittle fracture in the thin layer material takes place after inelastic strain only, using the necessary criterion (4) produces obvious result  $\theta_1^* = \theta_1^{(1)*} = \theta_2^{(1)*} = 0$ . The prefracture zone is located on the crack continuation and the critical load  $\sigma_{\infty 1}^0$  in terms of the necessary criterion is as follows

$$\sigma_{\infty 1}^0 / \sigma_{m1} = (k_1 / \sqrt{n_1}) \sqrt{r_1 / 2l_0}. \quad (12)$$

Relation (12) takes no account for strength properties of thin layers by the value  $\sigma_{\infty 1}^0$ .

Make use of the sufficient fracture criterion (5), (6), in which stress and strain fields are used when  $\theta_1^* = \theta_1^{(1)*} = \theta_2^{(1)*} = 0$ . Determine parameters of the critical opening  $2v_1^*$  of a macrocrack and the critical displacement  $2u_1^*$  of crack flanks, the thin layer thickness being neglected since  $r_2 \ll r_1$ . These critical parameters are determined through the prefracture zone width. Equate the plasticity zone width at the crack tip in the first material with the prefracture zone width, the prefracture zone in the first material occupying the rectangle with sides  $\Delta_1$  and  $a_1$ . Further the prefracture zone length  $\Delta_1$  is measured in  $r_1$ ,  $s = [\Delta_1 / r_1]$  being the integer part of  $\Delta_1 / r_1$ , i.e.,  $s$  is the number of fibers in the prefracture zone. Loading in the prefracture zone is properly such that these fibers are stretched (or compressed) under low-cycle loading mode. Using characteristics of the standard  $\sigma$ – $\varepsilon$  diagram and with account for plastic peculiarities of the first material, the critical macrocrack opening and the critical crack flank displacement can be written in the following form

$$2v_1^* = (5/4\pi)(\varepsilon_{11} - \varepsilon_{01})(K_{I\infty} / \sigma_{m1})^2, \quad K_{I\infty} = \sigma_{\infty} \sqrt{\pi l_0}, \quad 2u_1^* \equiv 0, \quad K_{II\infty} \equiv 0. \quad (13)$$

SIFs  $K_{I\Delta}$  and  $K_{II\Delta}$  generated by stresses  $\sigma_{m1}$  and  $\tau_{m1} \equiv 0$  can be presented in the form according to [12]

$$K_{I\Delta} = -\sigma_{m1} \sqrt{\pi l_0} [1 - (2/\pi) \arcsin(1 - \Delta_1 / l_0)], \quad K_{II\Delta} \equiv 0. \quad (14)$$

Emphasize that  $K_{I\Delta} < 0$ . Further the first class of solutions is considered when the total SIF  $K_I$  in relations (7) is positive, i.e.,  $K_I = K_{I\infty} + K_{I\Delta} > 0$ . Then for the first material, all parameters of criterion (5), (6) are determined by relations (7), (13), (14). After appropriate transformations, critical parameters  $\sigma_{\infty 1}^*$ ,  $\Delta_1^*$  are found from the first relations for criterion (5), (6). Assuming that  $\Delta_1^* / l^* \ll 1$ , these critical parameters  $\sigma_{\infty 1}^*$ ,  $\Delta_1^*$  can be written in the simple form

$$\frac{\Delta_1^*}{r_1} = \frac{k_1^2}{2n_1} \left[ \frac{5\sqrt{2}}{4(\eta+1)} \frac{G}{\sigma_{m1}} (\varepsilon_{11} - \varepsilon_{01}) \right]^2 \left[ 1 - \frac{5}{\pi(\eta+1)} \frac{G}{\sigma_{m1}} (\varepsilon_{11} - \varepsilon_{01}) \right]^{-2}, \quad (15)$$

$$\frac{\sigma_{\infty 1}^*}{\sigma_{m1}} = \sqrt{\frac{r_1}{2l^*}} \frac{k_1}{\sqrt{n_1}} \left[ 1 - \frac{5}{\pi(\eta+1)} \frac{G}{\sigma_{m1}} (\varepsilon_{11} - \varepsilon_{01}) \right]^{-1}. \quad (16)$$

For relations (15), (16), the following restriction is hold  $1 - (5/\pi)(\eta+1)^{-1} (G/\sigma_{m1})(\varepsilon_{11} - \varepsilon_{01}) > 0$ . Comparing relations (12) and (16) for critical loads, the following obvious inequality  $\sigma_{\infty 1}^* > \sigma_{\infty 1}^0$  is derived.

#### 4. Description of characteristics of fiber material under cyclic loading

Consider pulsating loading of a specimen with macrocrack. Fig. 5 displays the plot of one loading cycle where  $\sigma_a$  is the amplitude of loading and  $t$  is time. It is obvious that  $\sigma_{\infty 1}^0 < \sigma_a < \sigma_{\infty 1}^*$ , the amplitude  $\sigma_a$  in the low-cycle loading being commensurable with the critical load  $\sigma_{\infty 1}^*$ . Low-cycle fracture in the presence of macrocracks in the initial specimen is considered in the handbook [1]. Now strength characteristics of the fiber material under cyclic loading are considered. In Fig. 6 there are shown hysteresis loops for cyclically stable material. Further the simplest case is considered when the  $\sigma$ – $\varepsilon$  diagram possesses the complete symmetry, therefore all upper plus and minus signs are not used below.

Assume that under stationary pulsating loading  $\sigma_a = \text{const}$ , inelastic strain of material in a cycle is unchanged, i.e.,  $\varepsilon_\sigma = \varepsilon_\sigma(N) = \text{const}$  ( $N$  the number of cycle). To describe fracture of fibers ahead of the real macrocrack tip, make use of two approaches. Coffin [13] and his followers observed the relation between inelastic strain of material in a cycle and the number of cycles in experiments. In the simplest case, Coffin's equation has the form

$$N^{1/2} = C_1 / \varepsilon_\sigma, \quad (17)$$

where  $C_1$  is Coffin's constant that can be determined from monotonous loading as  $C_1 = \varepsilon_{11} / 2$ . The critical value of the number of cycles is determined for the first approach as

$$N_1^* = (\varepsilon_{11} / 2\varepsilon_\sigma)^2. \quad (18)$$

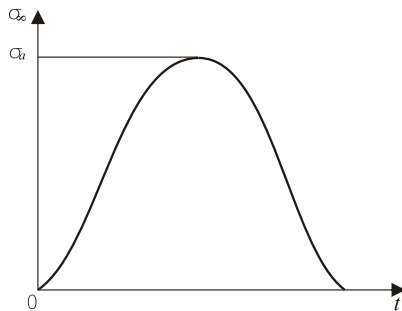


Fig. 5. Pulsating loading of specimen with macrocrack

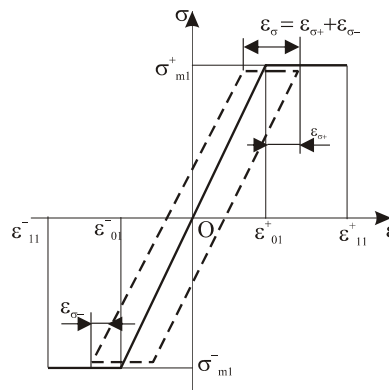


Fig. 6. Schematic  $\sigma$ – $\varepsilon$  diagrams for fiber material

In another approach [14], in order to account for damage accumulation in material of the prefailure zone, the notion of critical value of dissipated work at which the material is broken is introduced. This critical value is found experimentally. The critical value of the number of cycles  $N_2^*$  is determined from

$$N_2^* = \varepsilon_{11} / \varepsilon_\sigma, \quad (19)$$

where  $C_2 = O(1)$ ,  $1 \leq C_3 \leq 2$  are some constants, numerical values of which depend on peculiarities of fiber material;  $\varepsilon_\sigma$  is the parameter characterizing accumulation of damages per one cycle.



### 5. Accumulation of damages in the prefracture zone in high stress fatigue, hypothesis of cleavage crack arrest

The accumulation of damages under one loading cycle of the specimen with a macrocrack is associated with inelastic strain

$$\varepsilon_{\sigma} = \varepsilon_{\sigma+} + \varepsilon_{\sigma-} \quad (21)$$

of material of the fiber nearest to the middle of a macrocrack. The value of inelastic strain under tension  $\varepsilon_{\sigma+}$  depends on the level of loading  $\sigma_a$ . Explicit relations for  $\varepsilon_{\sigma+}$  and for the prefracture zone length  $\Delta_{l\sigma+}$  are obtained if  $\sigma_{\infty 1}^*$  is replaced by  $\sigma_a$ ,  $\varepsilon_{11} - \varepsilon_{01}$  is replaced by  $\varepsilon_{\sigma+}$ , and  $l^*$  is replaced by  $l$  in relations (15), (16). After transformations, we obtain

$$\varepsilon_{\sigma+} = \left( 1 - \frac{\sigma_a}{\sigma_{m1}} \sqrt{\frac{r_1}{2l}} \frac{k_1}{\sqrt{n_1}} \right) \left[ \frac{5}{\pi(\eta+1)} \frac{G}{\sigma_{m1}} \right]^{-1}, \quad (22)$$

$$\frac{\Delta_{l\sigma+}}{r_1} = \frac{k_1^2}{2n_1} \left( \frac{5\sqrt{2}}{4(\eta+1)} \frac{G}{\sigma_{m1}} \varepsilon_{\sigma+} \right)^2 \left( 1 - \frac{5}{\pi(\eta+1)} \frac{G}{\sigma_{m1}} \varepsilon_{\sigma+} \right)^{-2}. \quad (23)$$

For relations (22), (23), the restriction is imposed  $1 - (5/\pi)(\eta+1)^{-1} (G/\sigma_{m1}) \varepsilon_{\sigma+} > 0$ . Inelastic strain values under tension  $\varepsilon_{\sigma+}$  and prefracture zone lengths  $\Delta_{l\sigma+}$  depend on the amplitude of the load  $\sigma_a$  and the initial crack length since  $2l = 2l_0 + 2\Delta_{l\sigma+}$ , at that, if the dependence of  $\varepsilon_{\sigma+}$  on  $2l$  is weak, then the dependence of  $\Delta_{l\sigma+}$  on  $2l$  is much more pronounced. In repeated loading, materials in the prefracture zone are embrittled.

Further we consider only quasi-brittle fracture of fibers when the prefracture zone length is essentially less than the macrocrack length. i.e.,  $\Delta_{l\sigma+}/l \ll 1$ . When such restrictions are imposed, pulsating loading can be considered as rigid and the second summand in (21) vanishes, i.e.,  $\varepsilon_{\sigma-} \equiv 0$ . Thus we neglect residual stress and residual strains in the vicinity of the macrocrack tip after unloading in each cycle.

Make use of relation (20) for fiber material. The critical value of the number of cycles  $N^{*(1)}$  of material of the fiber nearest to the middle of the macrocrack of  $2l_0$  in length is determined from the relation

$$N^{*(j)} = C_2 \left( \varepsilon_{11} / \varepsilon_{\sigma+}^{(j)} \right)^{C_3}, \quad 2l^{(j)} = 2l^{(j-1)} + 2\Delta_{l\sigma+}^{(j)} \quad \text{for } j = 1, 2, 3, \dots, j^*; \quad l^{(0)} \equiv l_0. \quad (24)$$

Here  $N^{*(j)}$  and  $2l^{(j)}$  are critical values of the number of cycles and the macrocrack length, respectively,  $j^*$  is the total number of striations, for the first  $j=1$  and subsequent extensions of crack tips  $j=2, 3, 4, \dots$  such that  $N^{*(1)} \geq N^{*(2)} \geq \dots \geq N^{*(j^*)} = 1$ . The total number of loading cycles (fatigue life of specimen) is as follows

$$N^{\Sigma} = \sum_{j=1}^{j^*} N^{*(j)}. \quad (25)$$

After rupture of the fiber nearest to the middle of macrocrack in the prefracture zone, the geometry of macrocrack changes and the macrocrack is sharpened. Recall that mode I macrocrack is blunted due to occurrence of deformation ears. The new formed sharp macrocrack propagates through embrittled material in the prefracture zone. Embrittlement of materials is described by relations (3), which for mode I macrocrack transform to the relations

$$\varepsilon_{11}^{(i+1)} < \varepsilon_{11}^{(i)}, \varepsilon_{12}^{(i+2)} < \varepsilon_{12}^{(i+1)} \quad \text{for } i = 0, 1, 2, \dots, N^{(j)}; \quad j = 1, 2, 3, \dots, j^*. \quad (26)$$

Therefore, taking into consideration that after the fiber nearest to the middle of macrocrack is broken, the sharp macrocrack propagates through embrittled materials in accordance with (26). Let us formulate hypothesis of crack

arrest: the sharp crack of  $2l_0$  in length propagates only through embrittled materials, the crack extension by  $\Delta_{l\sigma+}^{(1)}$  is stepwise, and the crack stops at the boundary between fiber and thin layer. This thin layer is the first interlayer behind the prefracture zone. Further the process is repeated: in the next loading cycle  $N^{*(1)} + 1$ , the sharp crack of length  $2l^{(1)}$  is blunted due to occurrence of deformation ears, and in subsequent cycles, damages are accumulated in the modified prefracture zone, then in  $N^{*(1)} + N^{*(2)}$  loading cycle, stepwise extension of the crack of length  $2l^{(1)}$  in the modified prefracture zone  $\Delta_{l\sigma+}^{(2)}$  takes place, etc.

On average, the rate of macrocrack extension  $V = V(N)$  per one cycle is estimated if relations (22)–(24) are used

$$V = \Delta_{l\sigma+}^{(j)} / \left[ C_2 \left( \varepsilon_{11} / \varepsilon_{\sigma+}^{(j)} \right)^{C_3} \right] \quad \text{for } j = 1, 2, 3, \dots, j^* . \quad (27)$$

In relation (27), information about peculiarities of fiber material and characteristic of prefracture zone is used. As the crack length  $2l^{(j)}$  increases, the mean rate  $V = V(N)$  of crack extension essentially increases. This phenomenon is observed in experiments reported by Laird and Smith [2], Laird [3], and in handbook [1]. The proposed relations (22)–(25) describe the effect of failure of the specimen with a macrocrack when the crack length  $2l^{(j)}$  increases until the state when the specimen is broken into parts in the next loading cycle. After the specimen breaks up into parts,  $j^*$  striations ( $j^*$  tracks of ears) are observed on deformation surfaces.

## 6. Conclusions

The model of low-cycle fatigue describing extension of the crack tip in structured material is proposed. The initial crack is located perpendicular to fibers. The material is considered to consist of quasi-brittle fibers with thin layers, material of which is characterized by quasi-ductile type of fracture before strain, and after inelastic strain of thin layers, the fracture type changes to quasi-brittle. This model appropriate to the scheme by Laird and Smith [2] and describes occurrence of striations in fatigue. The detailed information about strain of material in the prefracture zone is obtained: processes of occurrence of deformation ears, healing of thin layer material, accumulation of damages in fibers, stepwise extension of the crack tip and failure of the specimen with a macrocrack are described. Simple relations for critical fracture parameters and fatigue time of the specimen are derived.

## Acknowledgements

The work was financially supported by Russian Foundation for Basic Research (Grant 07-01-00163) and in the context of the project No 11.16 included into the program of Presidium of Russian Academy of Sciences.

## References

- [1] Romaniv ON, Yarema SYa, Nikiforchin GN, Makhutov NA, Stadnik MM. Fatigue and cyclic fracture toughness of structural materials, Vol. 4. Fracture mechanics and strength of materials, in four volumes. Kiev: Naukova Dumka; 1990 (in Russian).
- [2] Laird C, Smith GC. Crack propagation in high stress fatigue. The Philosophical Magazine, A. Journal of Theor. Experim. and Applied Physics, 1962; 7, No. 77, 847-857.
- [3] Laird C. The influence of metallurgical structure on the mechanism of fatigue crack propagation. Fatigue Crack Propagation, ASTM STP 415; Am. Soc. Testing Mats., 1967; 131-168.
- [4] McClintock FA, Irwin GR. Plasticity aspects of fracture mechanics. In: Fracture toughness testing and its applications. SATM Special Technical Publication, 1965; No. 381, Am. Soc. Testing Mats., 84-113.
- [5] Kornev VM. Fracture of brittle and quasiductile crystals. Strength and deformation criteria. Applied Mathematics and Mechanics. 2003; 67, No. 6, 901-910.
- [6] Kornev VM. Branching and kink of opening crack paths in polycrystal. Physical Mesomechanics. 2003; 6, No. 5, 37-46 (in Russian).
- [7] Kornev VM. Rupture crack branching in solids with structural hierarchy. International Journal of Fracture. 2004; 128, No. 1, 205-214.

- [8] Kornev VM, Kurguzov VD. Multiparametric sufficient criterion of quasi-brittle fracture for complicated stress state. *Eng. Fracture Mechanics*. 2008; **75**, No. 5; 1099-1113.
- [9] Mikhailov SE.. A functional approach to non-local strength conditions and fracture criteria – II. Discrete fracture. *Eng. Fracture Mechanics*. 1995; **52**, No. 4, 745-754.
- [10] Novozhilov VV. About the necessary and sufficient brittle strength criteria. *Prikl. Mat. Mekh.* 1969; **33**, No. 2, 212-222 (in Russian).
- [11] Murakami Y. Stress intensity factors handbook (in 2 volumes), v. 1. Oxford, N.Y.:Pergamon Press;1986.
- [12] Savruk MP. Stress-intensity factor in cracked bodies, Vol. 2. Fracture mechanics and strength of materials, in four volumes. Kiev: Naukova Dumka; 1988 (in Russian).
- [13] Coffin LF, Schenectady NY. A Study of the effects of cyclic thermal stresses on a ductile metal. *Transations of the ASME*. 1954; **76**. No. 6, 931-950.
- [14] Nikitenko AF. Yield and long strength of metallurgical materials. Novosibirsk: Institute of Hydrodynamics, Siberian Branch of Russian Academy of Sciences; 1997 (in Russian).